



Published in final edited form as:

Neurosurgery. 2014 March ; 10(0 1): 74–83. doi:10.1227/NEU.000000000000117.

## 5-Aminolevulinic Acid-Induced Protoporphyrin IX Fluorescence in Meningioma: Qualitative and Quantitative Measurements In Vivo

Pablo A. Valdes, PhD<sup>\*,‡,§</sup>, Kimon Bekelis, MD<sup>\*</sup>, Brent T. Harris, MD, PhD<sup>||</sup>, Brian C. Wilson, PhD<sup>||</sup>, Frederic Leblond, PhD<sup>‡,#</sup>, Anthony Kim, PhD<sup>||</sup>, Nathan E. Simmons, MD<sup>\*</sup>, Kadir Erkmen, MD<sup>\*</sup>, Keith D. Paulsen, PhD<sup>‡,\*\*,†</sup>, and David W. Roberts, MD<sup>\*,§,††</sup>

<sup>\*</sup>Section of Neurosurgery, Dartmouth-Hitchcock Medical Center, Lebanon, New Hampshire

<sup>‡</sup>Thayer School of Engineering, Hanover, New Hampshire

<sup>§</sup>Geisel School of Medicine at Dartmouth, Hanover, New Hampshire

<sup>||</sup>Departments of Pathology and Neurology, Georgetown University Medical Center, Washington, DC

<sup>||</sup>Ontario Cancer Institute, University of Toronto, Toronto, Ontario, Canada

<sup>#</sup>Engineering Physics Department, École Polytechnique de Montreal, Montreal, Quebec, Canada

<sup>††</sup>Norris Cotton Cancer Center, Dartmouth-Hitchcock Medical Center, Lebanon, New Hampshire

### Abstract

**BACKGROUND**—The use of 5-aminolevulinic acid (ALA)-induced protoporphyrin IX (PpIX) fluorescence has shown promise as a surgical adjunct for maximizing the extent of surgical resection in gliomas. To date, the clinical utility of 5-ALA in meningiomas is not fully understood, with most descriptive studies using qualitative approaches to 5-ALA-PpIX.

**OBJECTIVE**—To assess the diagnostic performance of 5-ALA-PpIX fluorescence during surgical resection of meningioma.

**METHODS**—ALA was administered to 15 patients with meningioma undergoing PpIX fluorescence-guided surgery at our institution. At various points during the procedure, the surgeon performed qualitative, visual assessments of fluorescence by using the surgical microscope, followed by a quantitative fluorescence measurement by using an intra-operative probe. Specimens were collected at each point for subsequent neuropathological analysis. Clustered data analysis of variance was used to ascertain a difference between groups, and receiver operating characteristic analyses were performed to assess diagnostic capabilities.

**RESULTS**—Red-pink fluorescence was observed in 80% (12/15) of patients, with visible fluorescence generally demonstrating a strong, homogenous character. Quantitative fluorescence

Copyright © 2013 by the Congress of Neurological Surgeons.

**Correspondence:** David W. Roberts, MD, Dartmouth-Hitchcock Medical Center, Section of Neurosurgery, One Medical Center Dr, Lebanon, NH 03756. David.W.Roberts@dartmouth.edu or Pablo A. Valdes, PhD, Dartmouth-Hitchcock Medical Center, Section of Neurosurgery, One Medical Center Dr, Lebanon, NH 03756. Pablo.A.Valdes@dartmouth.edu.

measured diagnostically significant PpIX concentrations ( $C_{PpIX}$ ) in both visibly and nonvisibly fluorescent tissues, with significantly higher  $C_{PpIX}$  in both visibly fluorescent ( $P < .001$ ) and tumor tissue ( $P = .002$ ). Receiver operating characteristic analyses also showed diagnostic accuracies up to 90% for differentiating tumor from normal dura.

**CONCLUSION**—ALA-induced PpIX fluorescence guidance is a potential and promising adjunct in accurately detecting neoplastic tissue during meningioma resective surgery. These results suggest a broader reach for PpIX as a biomarker for meningiomas than was previously noted in the literature.

### Keywords

5-Aminolevulinic acid; Biophotonics; Brain tumor; Fluorescence-guided surgery; Meningioma  
Optical spectroscopy; Protoporphyrin IX

---

Meningiomas account for approximately 20%<sup>1</sup> of all intracranial tumors and, despite their benign nature, remain some of the most challenging neoplasms to treat. Completeness of tumor resection can offer a cure to patients, but achieving this goal can be difficult, especially in areas such as the skull base, given their proximity to and not infrequent invasion of dura, bony structures, major vessels, and cranial nerves.<sup>2,3</sup> Image guidance can assist in gross identification but may be limited by intraoperative loss of coregistration accuracy as well as imprecision in the delineation of sharp tumor borders.<sup>3</sup>

The use of 5-aminolevulinic acid (ALA)-induced protoporphyrin IX (PpIX) for fluorescence-guided resection (FGR) of malignant gliomas has shown promise as a tool in the neurosurgical armamentarium.<sup>4–12</sup> In brief, ALA is administered orally to the patient before surgery, which leads to the selective accumulation of a fluorescent compound, PpIX, in tumor cells.<sup>5,6,10,12,13</sup> PpIX can be detected by using violet-blue light excitation (excitation peak at 405 nm) and appropriate filters to detect the reemitted fluorescence (major emission peak at 635 nm).<sup>5,12–14</sup> FGR provides the surgeon with real-time feedback in the surgical field of view, with the red-pink fluorescence of PpIX assisting decision making with respect to the presence of tumor tissue.

Despite the curative nature of complete resection in meningiomas and the improved tumor delineation capabilities of ALA for FGR, few have reported its use for meningiomas,<sup>5,15–20</sup> with no consensus regarding its role in their resection. Most reports to date have used only a qualitative, visible fluorescence approach to FGR, which uses the visibly perceived red fluorescence from tissue to help guide decision making. We have recently shown that use of an intraoperative probe for quantitative fluorescence can detect diagnostically significant levels of PpIX across a range of tumor histologies beyond the capabilities of qualitative fluorescence, providing both an objective (ie, not prone to subjectivity due to variation in tissue optical properties that make the relationship between visual fluorescence and the actual levels of PpIX in tissue nonlinear) as well as highly sensitive approach to FGR.<sup>10,21–23</sup> This quantitative approach has shown promise as a complementary detection modality for use in ALA-PpIX FGR, but has not been thoroughly investigated in the context of FGR for meningiomas.

Here, we provide initial findings on 15 meningiomas undergoing ALA-induced PpIX FGR. We elaborate on the advantages and disadvantages of this fluorescence-guidance methodology as a surgical adjunct, providing a descriptive study on the use of PpIX fluorescence in meningioma surgery.

## MATERIALS AND METHODS

### Study Characteristics

All patients participating in this study were part of a broader prospective study of fluorescence-guided surgery.<sup>5,9,10</sup> The tumor resection protocol was approved by the Institutional Review Board of Dartmouth controlling the participation of human subjects in research, and all patients signed an informed consent. Inclusion and exclusion criteria have been reviewed in previous publications.<sup>5</sup> Patients were administered an oral dose of ALA (DUSA Pharmaceuticals, Tarrytown, New York), 20 mg/kg, dissolved in 100 mL of water approximately 3 hours before the induction of anesthesia. Preoperative, high-resolution contrast-enhanced T1-weighted axial images were acquired and used for image-guided neuronavigation.

### Surgical Procedure

Patients were positioned appropriately and their head was secured in 3-point fixation. A StealthStation Treon image-guidance system (Medtronic, Louisville, Colorado) was used for neuronavigation following standard practice. A Zeiss OPMI Pentero surgical microscope (Carl Zeiss Surgical GmbH, Oberkochen, Germany) modified for PpIX fluorescence guidance was coregistered with the surgical field using scalp fiducials. The Zeiss Pentero allows the surgeon to switch from standard white light illumination mode to violet-blue light mode (ie, fluorescence mode) to excite PpIX (excitation peak wavelength = 405 nm) and collect the remitted fluorescence (main PpIX emission wavelengths = 610–720 nm). Visualization is performed via the surgical oculars as well as on a color camera.<sup>5,9,10</sup>

The resection was performed following standard microsurgical technique with white light illumination of the surgical cavity. The surgeon alternated between white and violet-blue light modes to visualize fluorescence at several points during the resection. Biopsy specimens were collected at various times during surgery as well as in regions displaying both positive (ie, red-pink fluorescence) and negative (ie, no red-pink fluorescence) visible fluorescence within the preoperatively planned resection volume. Each tissue specimen was placed in formalin for subsequent histopathological analysis.<sup>5</sup>

Before biopsy acquisition, the surgeon placed a quantitative probe on the part of tissue to be biopsied and quantitative measurements were acquired in triplicate and averaged. Control data were acquired from normal dura. The site was assigned a qualitative visible fluorescence score from 0 to 3 (no, minimal, moderate, and high fluorescence, respectively) based on the impression of the surgeon who was blinded to the quantitative results. Resection was continued until the surgeon judged that no more tissue could be safely removed. Conventional neurosurgical technique with navigational guidance and white light illumination was the primary guide for resection, and only tissue within the planned

resection volume or judged to be abnormal was included. As an investigational procedure, tissue was not resected on the basis of fluorescence alone.<sup>10,24,25</sup> Postoperatively, to monitor possible changes in liver function and photosensitivity, all patients underwent serial liver function tests and were kept in a dark room for 3 days before discharge, respectively. At the time that this protocol was written, we chose a conservative time frame of 72 hours. The published literature supports a 24- to 48-hour time frame.

### Intraoperative Probe

We previously described a method using a quantitative intraoperative contact probe to perform in vivo measurements of the quantitative PpIX fluorescence in tissue in the resection of brain tumors across a broad range of tumor histologies.<sup>10,21,22</sup> The details on the technological implementation of the intraoperative probe have been provided in the following references by Valdes et al<sup>10,22</sup> and Kim et al.<sup>21</sup> The optical probe consists of 4 fiber optic cables linearly arranged and encased in a stainless steel housing approximately 1.1 mm in outer diameter. The fiber optics include 1 for light collection connected to a subnanometer resolution spectrometer, 2 for white light illumination at different distances from the detector fiber, and 1 for 405-nm excitation light illumination. The intraoperative probe system applies a light transport-modeling algorithm to the white light data to calculate the tissue optical properties and utilizes these data to correct the raw fluorescence for the variations in tissue light scattering and absorption.<sup>10,21,22,26</sup> This attenuation correction allows us to make quantitative assessments regarding the absolute levels of PpIX in tissue (ie,  $C_{PpIX}$ ), by correcting for the nonlinear, attenuating effects of varying optical properties.<sup>10,21,22,26,27</sup>

### Pathology

A neuropathologist (B.T.H.) blinded to the quantitative and qualitative measurements performed histopathological analysis on formalin-fixed, paraffin-embedded tissue. Each biopsy specimen was classified based on World Health Organization (WHO) grading criteria,<sup>28</sup> and data were tabulated matching each specimen with their corresponding histopathological results and their qualitative (ie, score 0–3) and quantitative fluorescence (ie,  $C_{PpIX}$ ) characteristics.

### Data and Statistical Analysis

Data processing was performed with the use of custom MATLAB software (Version R2011b, The Mathworks, Inc, Natick, Massachusetts). Stata 12.0 software (Stata Corporation, College Station, Texas) was used for statistical analyses. A Fisher exact test was used to ascertain an association between contrast enhancement, meningioma WHO grade, and visible fluorescence. Receiver operating characteristic (ROC) analyses were used to assess the diagnostic performance for both qualitative and quantitative fluorescence approaches as previously described. Given the multiple samples per patient, a robust generalized estimating equation model was used to perform a clustered data analysis of variance to ascertain a difference between groups, which is equivalent to a linear mixed model for random effects with fewer assumptions on data distribution (ie, no assumption of normality). The variance of the data measurements was estimated by calculating

$$\text{Var}_i = \frac{\sum (x_j - \mu_i)^2}{n - 1}$$

where  $\text{Var}_i$  is the variance at sample point  $i$ ,  $x_j$  is a single measurement estimate of  $C_{\text{PpIX}}$  for  $j = [1,2,3]$  of the triplicate measurements at sample point  $i$ , and  $\mu_i$  is the mean at sample point  $i$ , and  $n = 3$ . Two-sided  $P$  values of  $< .05$  are described as statistically significant in this study.

## RESULTS

### Patient Characteristics

Our study population included 15 patients with meningioma (11 WHO grade I and 4 WHO grade II). Two of the patients had recurrent tumors (both WHO grade II initially that remained grade II on recurrence) (Table 1). All 15 meningiomas were contrast-enhancing lesions on T1-weighted post-gadolinium injection magnetic resonance (MR) imaging. The mean patient age was 57.6 years (ranging from 28 to 84 years), with 6 men and 9 women (Table 1). No serious adverse events were recorded from the use of ALA in this study.

### Intraoperative Fluorescence

**General Impressions**—Eight of 11 patients with a grade I meningioma and all patients ( $n = 4$ ) with a grade II meningioma demonstrated visible levels of fluorescence. Overall, 80% of the patients demonstrated visible levels of fluorescence (Table 1). A two-by-two contingency table analysis using a Fisher exact test showed no statistically significant association between meningioma WHO grade and visible fluorescence in meningiomas ( $P = .52$ ).

Two prominent features of positive visible fluorescence were noted in our cohort of meningiomas. First, positive visible fluorescence in meningiomas was generally very high (ie, qualitative descriptors such as high<sup>5,9,10</sup> or strong visible fluorescence<sup>6,29</sup>) in character (Figure 1). A second feature was the homogenous character of positive visible fluorescence in meningiomas. When present, fluorescence in meningiomas generally demonstrated a more homogenous intratumoral visible fluorescence throughout the tumor, in contrast to the often highly heterogenous and “patchy” visible fluorescence observed in gliomas. It is important to note that different levels of PpIX fluorescence are found both inter- and intratumorally among meningiomas.<sup>5,15,19</sup> Both of these fluorescence features provide the surgeon a high contrast between tumor and adjacent tissue, allowing for a clear resection of tumor when visible fluorescence is present (Figure 1). Further, no visibly fluorescent tissue was observed in adjacent, edematous brain.

All meningiomas displayed contrast enhancement on preoperative T1-weighted MR imaging, and 3 did not show visible fluorescence. A two-by-two contingency table analysis using a Fisher exact test showed no statistically significant association between contrast enhancement on preoperative MR imaging and visible fluorescence in meningiomas ( $P = 1.00$ ).

Quantitative fluorescence with the use of the intraoperative probe was performed on 10 patients (Table 1) with a WHO I meningioma. Control points collected on normal dura in addition to all biopsied specimens interrogated by the probe were included in this analysis. A total of 49 interrogated sites from 10 meningiomas were used for analysis of absolute PpIX levels, with 16 control dura and 33 tumor tissue. Normal dura had an average  $C_{PpIX} = 0.006 \pm 0.003 \mu\text{g/mL}$  and median  $<0.001 \mu\text{g/mL}$  (interquartile range: 0.000–0.000), while tumor tissue had an average  $C_{PpIX} = 1.694 \pm 0.440 \mu\text{g/mL}$  and median  $0.705 \mu\text{g/mL}$  (interquartile range: 0.066–2.804) (Table 2). Tumor tissue showed a statistically significant increase ( $P = .002$ ) in  $C_{PpIX}$  levels compared with normal tissue (ie, normal dura). Further, PpIX levels in most normal dura (81.3%) (13/16 specimens) were less than the minimal detection limits of the system ( $<0.001 \mu\text{g/mL}$ ). Thirty-nine percent of confirmed tumor specimens (13/33) did not display visible levels of fluorescence; 69% of these specimens (9/13) contained PpIX levels greater than  $0.010 \mu\text{g/mL}$ . Absolute PpIX levels for the following categories: nonvisibly fluorescent tissue, visibly fluorescent tissue, nonvisibly fluorescent tumor tissue, nonvisibly fluorescent normal tissue, and visibly fluorescent tumor tissue are listed in Table 2. All visibly fluorescent tissue was tumor tissue. Normal tissue  $C_{PpIX}$  variance was calculated as median Var  $<0.001 \mu\text{g/mL}$  (minimum detection threshold,  $0.001 \mu\text{g/mL}$ ; interquartile range: 0.000–0.000), whereas tumor tissue  $C_{PpIX}$  variance was calculated as median Var =  $0.003 \mu\text{g/mL}$  (interquartile range: 0.000–0.558). Overall, median Var  $<0.001 \mu\text{g/mL}$  (interquartile range: 0.000–0.048).

**Capsule and Tumor Center**—Thirteen percent of patients (2/15) demonstrated a thick fibrous tumor capsule that did not demonstrate visible levels of fluorescence. Quantitative measurements showed both low (ie, below diagnostically significant levels,  $C_{PpIX} = 0.001$  and  $0.002 \mu\text{g/mL}$  in both patients) and high (ie, diagnostically significant levels,  $C_{PpIX} = 0.152 \mu\text{g/mL}$  in 1 patient) PpIX levels in these regions. Histopathology confirmed the presence of neoplastic tissue in all capsule tissue samples.

**Diagnostic Performance**—An ROC analysis on our cohort of 10 patients undergoing both quantitative and qualitative fluorescence was performed to test the diagnostic performance of qualitative fluorescence to correctly identify tissue, with visible impressions of fluorescence (positive visible red fluorescence or no visible fluorescence) used as a discriminatory variable, which demonstrated an ROC area under the curve (AUC) = 0.77, a classification efficiency = 71%, positive predictive value (PPV) = 0.95, specificity = 0.94, negative predictive value (NPV) = 0.55, and sensitivity = 0.61. An equivalent ROC analysis was performed to test the diagnostic performance of quantitative assessments of fluorescence for correctly identifying tissue, with  $C_{PpIX}$  used as a discriminatory variable. In our cohort of 10 meningiomas undergoing both quantitative and qualitative fluorescence guidance, with the use of a cutoff threshold of  $C_{PpIX} = 0.114 \mu\text{g/mL}$ , quantitative fluorescence demonstrated an ROC AUC = 0.93, a classification efficiency = 84%, PPV = 1.00, specificity = 1.00, NPV = 0.67, and sensitivity = 0.76 (Figure 2). With a cutoff threshold of  $c_{PpIX} = 0.001 \mu\text{g/mL}$  (ie, the point on the ROC curve closest to the upper left corner of the graph),<sup>30</sup> quantitative fluorescence demonstrated a classification efficiency = 90%, PPV = 0.91, specificity = 0.81, NPV = 0.87, and sensitivity = 0.94. The neurosurgeon can balance the need for improved sensitivity at the cost of decreased specificity, and vice



versa, by using a different cutoff threshold, and it is left to the surgeon's clinical judgment to be more aggressive (increased sensitivity) or more conservative (increased specificity). In summary, quantitative fluorescence demonstrated a highly statistically significant improvement in diagnostic performance compared with qualitative fluorescence following an ROC AUC comparison analysis ( $P = 0.007$ ) (Table 3).

## DISCUSSION

Meningiomas are likely to arise from arachnoidal cap cells, with likely extension to dura, and can be in proximity to cranial nerves and blood vessels.<sup>31,32</sup> In addition to involving critical functional anatomy, meningiomas can be associated with occult dural involvement, bone involvement, or peritumoral edema and brain invasion.<sup>33</sup> Attachments to gliotic brain, normal arteries, major sinuses, and the anterior visual pathways can be left behind and provide foci for recurrence.<sup>34–37</sup> The more extensive the involvement of these structures, the decreased likelihood of complete tumor resection, and the recurrence rate and operative morbidity increase.<sup>35–37</sup> Even in patients with the most extensive resection (Simpson grade I), an 8% 5-year recurrence rate has been reported because of residual tumor not detected during the initial operation.<sup>34</sup> To address this, aggressive resection of adjacent dura is usually attempted with margins often extending well beyond visible tumor.<sup>36–39</sup> This aggressive approach, however, has been challenged, suggesting that the radiographic dural tail can be normal edematous dura.<sup>40</sup>

Fluorescence-guided surgery using ALA-induced PpIX fluorescence has proven in recent years to be a powerful surgical adjunct for resection of high-grade gliomas.<sup>7,8,11,12</sup> Stummer et al,<sup>7</sup> in a phase III clinical trial, showed that use of ALA doubles the rate of complete resection and results in improved 6-month progression-free survival. These results demonstrate the utility of PpIX fluorescence in glioma surgery despite the highly invasive and infiltrative nature of gliomas. Building on Stummer's experience, Roberts et al, using a modified surgical microscope, demonstrated FGR with excellent positive predictive value for gliomas (0.95), but experienced significant sensitivity limitations (negative predictive value as low as 0.26). To address some of the limitations with current FGR, recent work has demonstrated with the use of a quantitative intraoperative probe a significant improvement in tumor detection across a range of tumor histologies—low- and high-grade glioma, meningioma, and metastases—compared with the more common qualitative approach. These results demonstrate the ability to detect imperceptible yet diagnostically significant levels of PpIX in tissue by using a more sensitive and objective approach.<sup>5,10,22,23</sup>

This study elaborates on the use of ALA-induced PpIX FGR in surgery for meningioma, reproducing previous results on visible PpIX fluorescence and incorporating quantitative fluorescence into the FGR armamentarium. Quantitative fluorescence demonstrates a broader and more significant reach of ALA-PpIX fluorescence in meningioma than previously thought. We highlight important imaging features of visible fluorescence as well as quantitative *in vivo* levels of PpIX with the use of an intraoperative probe, providing data that could potentially be used to tailor the extent of resection to the true extent of the disease. FGR could prove to be a powerful surgical adjunct in meningiomas, which constitute approximately one-fifth of primary intracranial neoplasms, and their benign,

noninfiltrative nature enables a cure when complete resection of tumor can be achieved.<sup>41</sup> Image guidance may be less important in extra-axial surgery, such as meningioma resection, but can facilitate gross tumor recognition and differentiation from normal structures. Although this is usually sufficient, there are some locations, such as the dural margin, close to the venous sinuses or the skull base, where the attempt to preserve normal structures can result in residual microscopic disease that can be the basis for tumor recurrence.

The literature contains a few initial experiences using ALA-induced PpIX fluorescence for meningioma resection. Coluccia et al<sup>15</sup> reported that 94% of their patients with meningiomas demonstrated visible fluorescence. Kajimoto et al<sup>16</sup> reported the sensitivity and specificity of PpIX fluorescence of the main tumor mass to be 83% and 100%, respectively. The authors reported that fluorescence assisted in surgical decision making and resulted in more complete resections. Moreover, Morofuji et al<sup>17</sup> reported the use of PpIX fluorescence in areas of bone invasion in a convexity meningioma and successfully correlated those with postoperative histological findings. The Dartmouth group has previously shown the use of PpIX fluorescence for both a falx and a skull base meningioma. The former demonstrated significant PpIX fluorescence in the dural tail under confocal microscopy analysis,<sup>20</sup> and, in the latter skull base meningioma, the authors presented their first experience using a quantitative spectroscopy probe to detect diagnostically significant quantitative levels (ie, concentration) of PpIX.<sup>5</sup> In summary, most of the initial studies to date on meningiomas and ALA have used a qualitative approach to fluorescence guidance, providing preliminary evidence for the utility of FGR for meningioma, where recurrence and eventually cure depend on the completeness of resection.

This work presents a cohort of 15 patients with a meningioma undergoing FGR. In the present study, visible fluorescence was observed in 80% of cases and, when present, displayed a characteristic high signal intensity and fairly homogenous distribution throughout the tumor. In 3 of 15 patients, no visible fluorescence was noted throughout the whole tumor. These results are consistent with previous literature reports from Coluccia et al<sup>15</sup> and Kajimoto et al<sup>16</sup> in terms of proportion of tumors with positive levels of visible PpIX fluorescence, noting the utility of this technique in 80% to 90% of meningiomas with the use of a visible fluorescence technique only.

These 2 previous reports did not comment on the absolute levels of PpIX in both visibly and nonvisibly fluorescent tissue and its impact on adequately detecting tumor tissue. We have<sup>10</sup> previously reported on 6 meningiomas using the quantitative intraoperative probe, with a classification efficiency = 97%, AUC = 0.98, sensitivity = 100%, NPV = 100%, specificity = 93%, and PPV = 95% with a cutoff value of  $C_{PpIX} > 0.010 \mu\text{g/mL}$ . This study shows slightly decreased, yet consistent results in terms of improved diagnostic accuracy in a larger cohort of patients with a classification efficiency = 90%, AUC = 0.93, sensitivity = 94%, NPV = 87%, specificity = 81%, and PPV = 91% with a cutoff value of  $C_{PpIX} > 0.001 \mu\text{g/mL}$ . Further, quantitative fluorescence detected diagnostically significant levels of PpIX (ie,  $C_{PpIX} > 0.010 \mu\text{g/mL}$ ) in 69% of histologically confirmed instances of tumor tissue with no visible fluorescence. Previous studies did not investigate quantitative assessments of PpIX as a tissue biomarker in histologically confirmed tumor tissue with no visible fluorescence (ie, false negatives). In a broader context, these results demonstrate that ALA-PpIX FGR is



not limited to just visibly fluorescent meningiomas. It is of interest to note that, in 2 cases where visible fluorescence was observed, the tumor capsule was always negative for visible fluorescence. In all instances, the capsule biopsy samples were histopathologically confirmed tumor tissue, with 1 sample showing significantly high levels of  $C_{PpIX} = 0.152$   $\mu\text{g/mL}$ .

A limitation of this study involves sampling bias inherent in the methodology as a result of the limited ability to perform probe measurements and histopathology on every section of tumor. The authors acknowledge this, and took measures to limit the impact of sampling bias, including acquiring multiple biopsies per patient at the beginning, middle, and end of surgery,<sup>5,10</sup> and acquiring samples from areas with both positive ( $n = 20$ ) and no visible fluorescence ( $n = 29$ ). The accrual of additional patients should help strengthen these findings. Further, future studies will describe the distinct  $C_{PpIX}$  levels found in various normal intracranial tissues, eg, normal white and gray matter, pia, bone, with previously reported values of  $<0.01$   $\mu\text{g/mL}$ .<sup>10</sup>

Attempts to predict the histological characteristics of meningiomas on the basis of imaging studies have yielded varied results. Most consistently, several studies have demonstrated that higher T2 signal intensity is associated with more vascular tumors.<sup>42–47</sup> There has been no association of T1 signal intensity and histological subtype of the tumor.<sup>42–47</sup> No correlation between the degree of MRI contrast enhancement and the histopathological features, vascularity, or consistency of intracranial meningiomas has been identified. This is in agreement with similar findings in studies based on computed tomography (CT).<sup>47</sup> In our study, patients demonstrated contrast enhancement on post-gadolinium injection T1-weighted images. We found no correlation between global assessment of contrast enhancement and PpIX fluorescence. In gliomas we observed a high correlation between contrast enhancement<sup>5,11,48</sup> and quantitative levels of gadolinium in ex vivo biopsies and (quantitative and qualitative) PpIX fluorescence,<sup>49</sup> suggesting the importance of increased delivery of ALA substrate to already metabolically active (tumor) tissue. It is important to note that the high, homogenous visible fluorescence observed in meningiomas might in part be attributed to the unimpaired delivery of ALA to tumor tissue, as evidenced by contrast enhancement. Recent work suggests a significant role for ferrochelatase, an enzyme involved in converting PpIX to heme by the addition of an iron atom, in explaining the differential accumulation of PpIX levels in tissue,<sup>50–52</sup> and specifically, meningioma cells.<sup>53</sup> The present study did not seek to address the relationship between PpIX fluorescence and MR imaging features in meningiomas and was not sufficiently powered to detect this. Future work will seek to understand the biological basis for PpIX accumulation in meningiomas. Recent work by Hefti et al.<sup>53</sup> showed that a difference in ferrochelatase activity may be a significant factor in PpIX accumulation in meningioma tumor cells. These results are in agreement with previous studies positing a significant role between ferrochelatase, iron availability, and PpIX accumulation.<sup>51,52,54</sup>

One limitation of this study was the cohort size of 15 meningiomas, which limited the ability to draw significant conclusions between meningioma subtypes and PpIX fluorescence as well as between contrast enhancement on MRI and PpIX fluorescence. Previous work has shown a strong correlation between measures of tumor aggressiveness and both qualitative

and quantitative PpIX fluorescence in larger cohorts of gliomas.<sup>5,9</sup> The present study did not seek to address the relationship between qualitative fluorescence intensity or quantitative levels of PpIX and tumor histopathology.<sup>19</sup> Further, this work did not explicitly address the ability of the probe to identify the resection margin at the tumor-normal dura interface. The results presented here demonstrate the ability to detect diagnostic nanogram levels of PpIX. Previous work<sup>20</sup> showed a strong correlation between PpIX fluorescence and the resection margin in a recurrent meningioma at the micrometer level. A sensitive tool such as the quantitative probe would be able to detect down to nanogram levels of PpIX but would be limited by the spatial resolution of the probe tip (1 mm in diameter). Another limitation involves the use of a small (~ 1 mm in diameter) contact quantitative probe, which limits the area of interrogated tissue and requires multiple sampling by the surgeon to assess quantitative levels of PpIX across the field of view. Our group recently developed a wide-field, quantitative fluorescence imaging system that seamlessly integrates into modern neurosurgical microscopes (eg, Zeiss Pentero) and provides highly sensitive, wide-field images of  $c_{PpIX}$  across the surgical field of view.<sup>23-25</sup> We plan to implement the new imaging system on future meningioma surgeries. Further, the ROC studies were both limited in number (49 specimens) and also suffered from selection bias in site and specimen assessment. In the current study, the prevalence of disease (ie, the total number of abnormal tumor sites interrogated divided by the total number of both normal and abnormal sites) was high.<sup>24,55</sup> Under certain assumptions, the sensitivity and specificity are independent of disease prevalence. Meanwhile, predictive values are highly dependent on disease prevalence. Given that this technique is intended for use in patients with a presumed preoperative diagnosis of meningioma, disease prevalence will always be high, and, as such, the expected predictive values would be expected to remain diagnostically high.<sup>24</sup> Nevertheless, the analysis of the diagnostic capabilities of PpIX fluorescence can inform the reader regarding the potential of this imaging technique for surgical guidance.

## CONCLUSION

Effective treatment of meningiomas requires complete resection of tumor, and this is imperative to prevent recurrence. ALA-induced PpIX fluorescence could serve as a tool to help delineate neoplastic tissue, highlight invasive regions, and tailor the extent of tumor resection to avoid destruction of normal surrounding tissue. Here, we elaborated on the use of ALA-induced PpIX FGR in a cohort of 15 meningiomas. Visual, qualitative fluorescence provides real-time delineation of regions with high levels of PpIX (~>0.500  $\mu\text{g}/\text{mL}$ ), allowing the surgeon to use the characteristic red-pink fluorescence from PpIX for guidance. A quantitative approach serves a complementary role by helping identify occult tumor regions containing nonvisibly fluorescent but diagnostically significant levels of PpIX, thus helping improve the sensitivity of PpIX FGR. These results show that PpIX FGR can serve as a surgical adjunct to standard white light image-guided resection, maximizing therapeutic effect and minimizing complications in the treatment of meningioma.

## Acknowledgments

### Disclosure

This work was supported in part by NIH grant R01NS052274-01A2 to 04 (D.W.R.) awarded by the National Institute of Neurological Disorders and Stroke. Carl Zeiss (Carl Zeiss Surgical GmbH, Oberkochen, Germany) and Medtronic Navigation (Medtronic, Louisville, Colorado) provided the fluorescence-enabled OPMI Penetro operating microscope and StealthStation Treon navigation system, respectively. DUSA Pharmaceuticals (DUSA Pharmaceuticals, Tarrytown, New York) supplied the ALA. Dr Roberts served as a consultant for Medtronic Think Tanks (2012), for Zeiss Think Tanks (2012 and 2013), for a Scientific Advisory Board for an unrelated Alcyone study, for a Scientific Advisory Board for an unrelated IMRIS/ SYMBIS study, for Zeiss's Neurosurgery Advisory Board, and on the Data Monitoring Committee for an unrelated Medtronic deep brain stimulation study. Drs Kim, Wilson, Valdes, Paulsen, and Roberts have 2 patent applications on several aspects of the quantitative fluorescence technologies discussed in this study.

## ABBREVIATIONS

<b>ALA</b>	5-aminolevulinic acid
<b>AUC</b>	area under the curve
<b>FGR</b>	fluorescence-guided resection
<b>NPV</b>	negative predictive value
<b>PpIX</b>	protoporphyrin IX
<b>PPV</b>	positive predictive value
<b>ROC</b>	receiver operating characteristic
<b>WHO</b>	World Health Organization

## REFERENCES

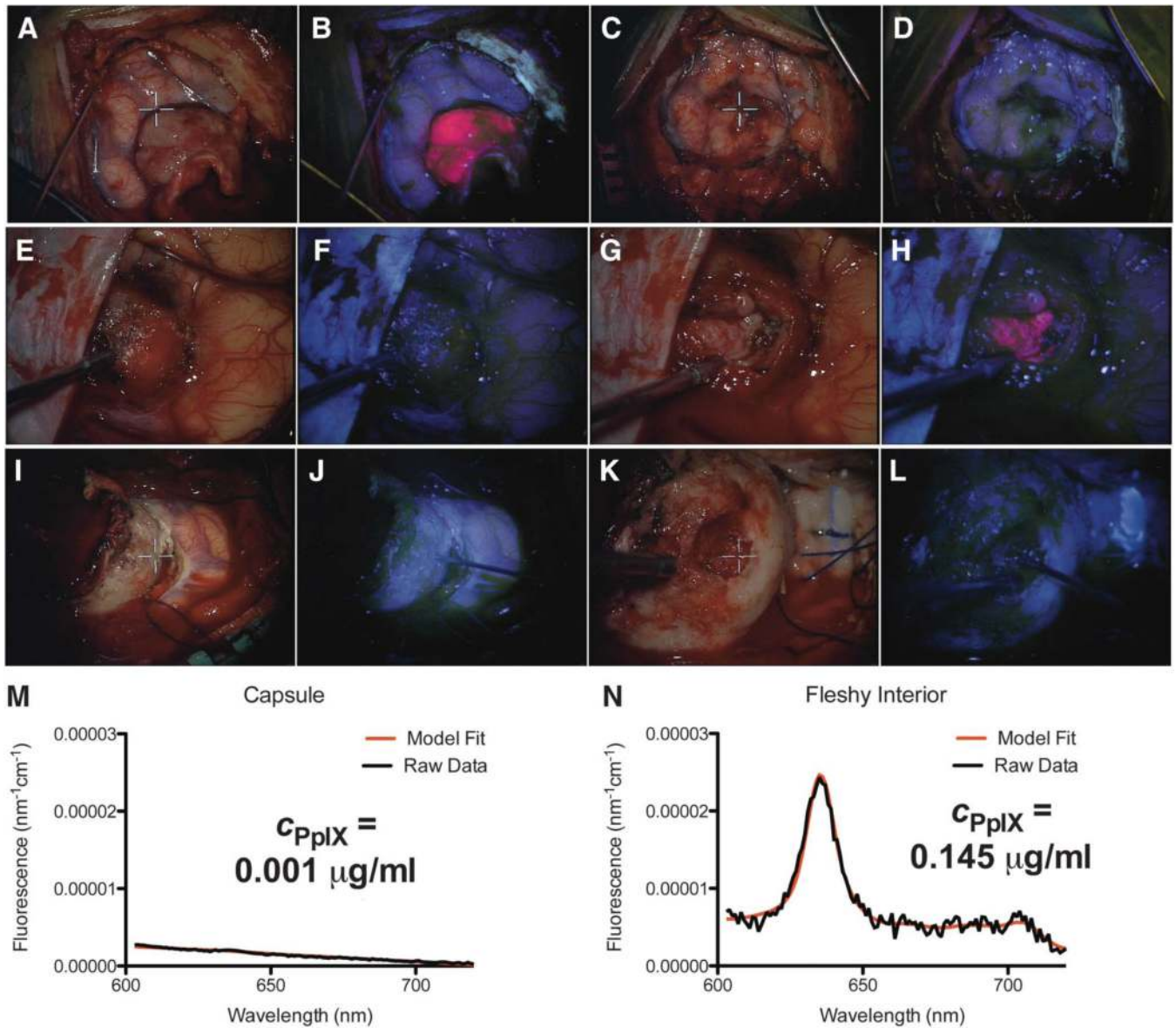
1. DeAngelis LM. Brain tumors. *N Engl J Med*. 2001; 344(2):114–123. [PubMed: 11150363]
2. Bulsara KR, Al-Mefty O. Skull base surgery for benign skull base tumors. *J Neurooncol*. 2004; 69(1–3):181–189. [PubMed: 15527089]
3. Samii M, Gerganov VM. Surgery of extra-axial tumors of the cerebral base. *Neurosurgery*. 2008; 62(6 suppl 3):1153–1166. [PubMed: 18695537]
4. Nabavi A, Thurm H, Zountsas B, et al. Five-aminolevulinic acid for fluorescence-guided resection of recurrent malignant gliomas: a phase ii study. *Neurosurgery*. 2009; 65(6):1070–1076. discussion 1076–1077. [PubMed: 19934966]
5. Bekelis K, Valdés PA, Erkmen K, et al. Quantitative and qualitative 5-aminolevulinic acid-induced Protoporphyrin IX fluorescence in skull base meningiomas. *Neurosurg Focus*. 2011; 30(5):E8. [PubMed: 21529179]
6. Stummer W, Novotny A, Stepp H, Goetz C, Bise K, Reulen HJ. Fluorescence-guided resection of glioblastoma multiforme by using 5-aminolevulinic acid-induced porphyrins: a prospective study in 52 consecutive patients. *J Neurosurg*. 2000; 93(6):1003–1013. [PubMed: 11117842]
7. Stummer W, Pichlmeier U, Meinel T, Wiestler OD, Zanella F, Reulen HJ. Fluorescence-guided surgery with 5-aminolevulinic acid for resection of malignant glioma: a randomised controlled multicentre phase III trial. *Lancet Oncol*. 2006; 7(5):392–401. [PubMed: 16648043]
8. Stummer W, Reulen HJ, Meinel T, et al. Extent of resection and survival in glioblastoma multiforme: identification of and adjustment for bias. *Neurosurgery*. 2008; 62(3):564–576. discussion 564–576. [PubMed: 18425006]
9. Valdes PA, Kim A, Brantsch M, et al.  $\delta$ -aminolevulinic acid-induced protoporphyrin IX concentration correlates with histopathologic markers of malignancy in human gliomas: the need for quantitative fluorescence-guided resection to identify regions of increasing malignancy. *Neuro Oncol*. 2011; 13(8):846–856. [PubMed: 21798847]
10. Valdés PA, Leblond F, Kim A, et al. Quantitative fluorescence in intracranial tumor: implications for ALA-induced PpIX as an intraoperative biomarker. *J Neurosurg*. 2011; 115(1):11–17. [PubMed: 21438658]

11. Roberts DW, Valdés PA, Harris BT, et al. Glioblastoma multiforme treatment with clinical trials for surgical resection (aminolevulinic acid). *Neurosurg Clin N Am.* 2012; 23(3):371–377. [PubMed: 22748650]
12. Valdes PA, Jacobs VL, Paulsen KD, Roberts DW, Leblond F. In vivo fluorescence detection in surgery: a review of principles, methods, and applications. *Curr Med Imaging Rev.* 2012; 8(3): 211–232.
13. Pogue BW, Gibbs-Strauss S, Valdés PA, Samkoe K, Roberts DW, Paulsen KD. Review of neurosurgical fluorescence imaging methodologies. *IEEE J Sel Top Quantum Electron.* 2010; 16(3):493–505. [PubMed: 20671936]
14. Stummer W, Stepp H, Möiler G, Ehrhardt A, Leonhar M, Reulen HJ. Technical principles for protoporphyrin-IX-fluorescence guided microsurgical resection of malignant glioma tissue. *Acta Neurochir (Wien).* 1998; 140(10):995–1000. [PubMed: 9856241]
15. Coluccia D, Fandino J, Fujioka M, Cordovi S, Muroi C, Landolt H. Intraoperative 5-aminolevulinic-acid-induced fluorescence in meningiomas. *Acta Neurochir (Wien).* 2010; 152(10):1711–1719. [PubMed: 20535506]
16. Kajimoto Y, Kuroiwa T, Miyatake S, et al. Use of 5-aminolevulinic acid in fluorescence-guided resection of meningioma with high risk of recurrence. Case report. *J Neurosurg.* 2007; 106(6): 1070–1074. [PubMed: 17564181]
17. Morofuji Y, Matsuo T, Hayashi Y, Suyama K, Nagata I. Usefulness of intraoperative photodynamic diagnosis using 5-aminolevulinic acid for meningiomas with cranial invasion: technical case report. *Neurosurgery.* 2008; 62(3 suppl 1):102–103. [PubMed: 18424972]
18. Tsai JC, Hsiao YY, Teng LJ, Chen CT, Kao MC. Comparative study on the ALA photodynamic effects of human glioma and meningioma cells. *Lasers Surg Med.* 1999; 24(4):296–305. [PubMed: 10327048]
19. Hefti M. Comment concerning: intraoperative 5-aminolevulinic-acid-induced fluorescence in meningiomas, *Acta Neurochir* DOI 10.1007/s00701-010-0708-4, Intratumoral heterogeneity and fluorescence intensity in meningioma after 5-ALA pretreatment. *Acta Neurochir (Wien).* 2011; 153(4):959–960. [PubMed: 21279659]
20. Whitson WJ, Valdes PA, Harris BT, Paulsen KD, Roberts DW. Confocal microscopy for the histological fluorescence pattern of a recurrent atypical meningioma: case report. *Neurosurgery.* 2011; 68(6):E1768–E1772. discussion E1772–E1773. [PubMed: 21389893]
21. Kim A, Khurana M, Moriyama Y, Wilson BC. Quantification of in vivo fluorescence decoupled from the effects of tissue optical properties using fiber-optic spectroscopy measurements. *J Biomed Opt.* 2010; 15(6):067006. [PubMed: 21198210]
22. Valdés PA, Kim A, Leblond F, et al. Combined fluorescence and reflectance spectroscopy for in vivo quantification of cancer biomarkers in low- and high-grade glioma surgery. *J Biomed Opt.* 2011; 16(11):116007. [PubMed: 22112112]
23. Valdés PA, Leblond F, Kim A, Wilson BC, Paulsen KD, Roberts DW. A spectrally constrained dual-band normalization technique for protoporphyrin IX quantification in fluorescence-guided surgery. *Opt Lett.* 2012; 37(11):1817–1819. [PubMed: 22660039]
24. Roberts DW, Valdés PA, Harris BT, et al. Coregistered fluorescence-enhanced tumor resection of malignant glioma: relationships between  $\delta$ -aminolevulinic acid-induced protoporphyrin IX fluorescence, magnetic resonance imaging enhancement, and neuropathological parameters. Clinical article. *J Neurosurg.* 2011; 114(3):595–603. [PubMed: 20380535]
25. Valdés PA, Leblond F, Jacobs VL, Wilson BC, Paulsen KD, Roberts DW. Quantitative, spectrally-resolved intraoperative fluorescence imaging. *Sci Rep.* 2012; 2:798. [PubMed: 23152935]
26. Kim A, Roy M, Dadani F, Wilson BC. A fiberoptic reflectance probe with multiple source-collector separations to increase the dynamic range of derived tissue optical absorption and scattering coefficients. *Opt Express.* 2010; 18(6):5580–5594. [PubMed: 20389574]
27. Bradley RS, Thorniley MS. A review of attenuation correction techniques for tissue fluorescence. *J R Soc Interface.* 2006; 3(6):1–13. [PubMed: 16849213]
28. Louis DN, Ohgaki H, Wiestler OD, et al. The 2007 WHO classification of tumours of the central nervous system. *Acta Neuropathol.* 2007; 114(2):97–109. [PubMed: 17618441]

29. Stummer W, Stocker S, Wagner S, et al. Intraoperative detection of malignant gliomas by 5-aminolevulinic acid-induced porphyrin fluorescence. *Neurosurgery*. 1998; 42(3):518–525. discussion 525–526. [PubMed: 9526986]
30. Shapiro DE. The interpretation of diagnostic tests. *Stat Methods Med Res*. 1999; 8(2):113–134. [PubMed: 10501649]
31. Buetow MP, Buetow PC, Smirniotopoulos JG. Typical, atypical, and misleading features in meningioma. *Radiographics*. 1991; 11(6):1087–1106. [PubMed: 1749851]
32. Kalamarides M, Stemmer-Rachamimov AO, Niwa-Kawakita M, et al. Identification of a progenitor cell of origin capable of generating diverse meningioma histological subtypes. *Oncogene*. 2011; 30(20):2333–2344. [PubMed: 21242963]
33. Jääskeläinen J, Haltia M, Servo A. Atypical and anaplastic meningiomas: radiology, surgery, radiotherapy, and outcome. *Surg Neurol*. 1986; 25(3):233–242. [PubMed: 3945904]
34. Ayerbe J, Lobato RD, de la Cruz J, et al. Risk factors predicting recurrence in patients operated on for intracranial meningioma. A multivariate analysis. *Acta Neurochir (Wien)*. 1999; 141(9):921–932. [PubMed: 10526073]
35. Jääskeläinen J. Seemingly complete removal of histologically benign intracranial meningioma: late recurrence rate and factors predicting recurrence in 657 patients. A multivariate analysis. *Surg Neurol*. 1986; 26(5):461–469. [PubMed: 3764651]
36. Nakasu S, Nakasu Y, Nakajima M, Matsuda M, Handa J. Preoperative identification of meningiomas that are highly likely to recur. *J Neurosurg*. 1999; 90(3):455–462. [PubMed: 10067913]
37. Al-Mefty O, Kadri PA, Pravdenkova S, Sawyer JR, Stangeby C, Husain M. Malignant progression in meningioma: documentation of a series and analysis of cytogenetic findings. *J Neurosurg*. 2004; 101(2):210–218. [PubMed: 15309910]
38. Borovich B, Doron Y. Recurrence of intracranial meningiomas: the role played by regional multicentricity. *J Neurosurg*. 1986; 64(1):58–63. [PubMed: 3941351]
39. Kinjo T, al-Mefty O, Kanaan I. Grade zero removal of supratentorial convexity meningiomas. *Neurosurgery*. 1993; 33(3):394–399. [PubMed: 8413869]
40. Kawahara Y, Niiro M, Yokoyama S, Kuratsu J. Dural congestion accompanying meningioma invasion into vessels: the dural tail sign. *Neuroradiology*. 2001; 43(6):462–465. [PubMed: 11465757]
41. Bondy M, Ligon BL. Epidemiology and etiology of intracranial meningiomas: a review. *J Neurooncol*. 1996; 29(3):197–205. [PubMed: 8858525]
42. Chen TC, Zee CS, Miller CA, et al. Magnetic resonance imaging and pathological correlates of meningiomas. *Neurosurgery*. 1992; 31(6):1015–1021. discussion 1021–1022. [PubMed: 1281915]
43. Maiuri F, Iaconetta G, de Divitiis O, Cirillo S, Di Salle F, De Caro ML. Intracranial meningiomas: correlations between MR imaging and histology. *Eur J Radiol*. 1999; 31(1):69–75. [PubMed: 10477102]
44. Ildan F, Tuna M, Göçer AP, et al. Correlation of the relationships of brain-tumor interfaces, magnetic resonance imaging, and angiographic findings to predict cleavage of meningiomas. *J Neurosurg*. 1999; 91(3):384–390. [PubMed: 10470811]
45. Elster AD, Challa VR, Gilbert TH, Richardson DN, Contento JC. Meningiomas: MR and histopathologic features. *Radiology*. 1989; 170(3 pt 1):857–862. [PubMed: 2916043]
46. Carpeggiani P, Crisi G, Trevisan C. MRI of intracranial meningiomas: correlations with histology and physical consistency. *Neuroradiology*. 1993; 35(7):532–536. [PubMed: 8232883]
47. Kendall B, Pullicino P. Comparison of consistency of meningiomas and CT appearances. *Neuroradiology*. 1979; 18(4):173–176. [PubMed: 530427]
48. Valdés PA, Fan X, Ji S, Harris BT, Paulsen KD, Roberts DW. Estimation of brain deformation for volumetric image updating in protoporphyrin IX fluorescence-guided resection. *Stereotact Funct Neurosurg*. 2010; 88(1):1–10. [PubMed: 19907205]
49. Valdés PA, Moses ZB, Kim A, et al. Gadolinium- and 5-aminolevulinic acid-induced protoporphyrin IX levels in human gliomas: an ex vivo quantitative study to correlate protoporphyrin IX levels and blood-brain barrier breakdown. *J Neuropathol Exp Neurol*. 2012; 71(9):806–813. [PubMed: 22878664]

50. Collaud S, Juzeniene A, Moan J, Lange N. On the selectivity of 5-aminolevulinic acid-induced protoporphyrin IX formation. *Curr Med Chem Anticancer Agents*. 2004; 4(3):301–316. [PubMed: 15134506]
51. Curnow A, Pye A. Biochemical manipulation via iron chelation to enhance porphyrin production from porphyrin precursors. *Environ Pathol Toxicol Oncol*. 2007; 26(2):89–103.
52. Valdes PA, Samkoe K, O'Hara JA, Roberts DW, Paulsen KD, Pogue BW. Deferoxamine iron chelation increases delta-aminolevulinic acid induced protoporphyrin IX in xenograft glioma model. *Photochem Photobiol*. 2010; 86(2):471–475. [PubMed: 20003159]
53. Hefti M, Hostenstein F, Albert I, Looser H, Luginbuehl V. Susceptibility to 5-aminolevulinic acid based photodynamic therapy in WHO I meningioma cells corresponds to ferrochelatase activity. *Photochem Photobiol*. 2011; 87(1):235–241. [PubMed: 21073472]
54. Blake E, Allen J, Curnow A. An in vitro comparison of the effects of the iron-chelating agents, CP94 and dexrazoxane, on protoporphyrin IX accumulation for photodynamic therapy and/or fluorescence guided resection. *Photochem Photobiol*. 2011; 87(6):1419–1426. [PubMed: 21834866]
55. Brenner H, Gefeller O. Variation of sensitivity, specificity, likelihood ratios and predictive values with disease prevalence. *Stat Med*. 1997; 16(9):981–991. [PubMed: 9160493]



**FIGURE 1.**

PpIX fluorescence in meningiomas **A** to **D** patient 1, 71-year-old man with a WHO I meningioma. Intraoperative images prior to tumor removal under white light (**A**) and visual fluorescence mode (**B**), and following tumor removal under white light (**C**) and fluorescence mode (**D**), demonstrate resection of tumor and no remnant amounts of visibly fluorescent tissue **E** to **H**, patient 2, 65-year-old woman with an atypical WHO II meningioma. Intraoperative view under white light (**E**) and fluorescence mode (**F**) on the surface of the tumor capsule, showing no visible fluorescence, and deep to the capsule within the fleshy tumor center under white light (**G**) and fluorescence mode (**H**), showing strong visible fluorescence **I** to **N** patient 3, 80-year-old man with a WHO I meningioma. Intraoperative view of tumor capsule under white light (**I**) and fluorescence mode (**J**), with a probe acquisition at the capsule surface; and corresponding white light (**K**) and fluorescence images (**L**) deep to capsule with a probe acquisition in the tumor bulk. Spectral readings at

capsule (**M**) show no significant PpIX levels, and only associated autofluorescence in tissue, whereas **N** shows significant signal and corresponding high levels of accumulated PpIX in the visually nonfluorescent tumor bulk. PpIX, protoporphyrin IX; WHO, World Health Organization.

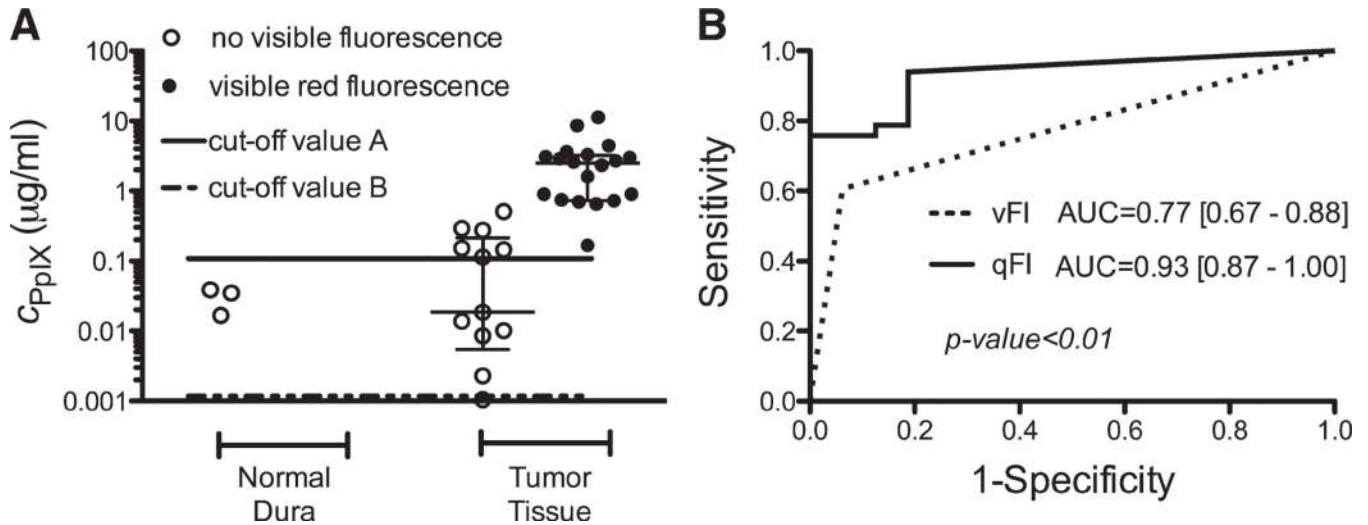


**FIGURE 2.**

Relationships between quantitative and qualitative fluorescence **A** scatter plot of specimens showing nonvisible (open circles) and visible (closed circles) fluorescence and their quantitative levels of PpIX separated into normal and tumor tissue, with a significant difference between visible and nonvisibly fluorescent ( $P < .001$ ) and between normal and tumor tissue ( $P = .002$ ). Error bars denote median and interquartile range. Two different cutoffs with either improved specificity (solid line, **A**) or improved sensitivity (dashed line, **B**) **B** ROC curves for qualitative fluorescence (vFI, dotted line) and quantitative fluorescence (qFI, solid line) showed a statistically significant difference in the ROC AUC for quantitative fluorescence ( $P < .01$ ). Sixteen data points are not shown that fell below  $< 0.001 \mu\text{g/mL}$ , with 13/16 histopathologically confirmed as normal dura. AUC, area under the curve; PpIX, protoporphyrin IX; ROC, receiver operating characteristic.

**TABLE 1**

Characteristics on 15 Patients With Meningioma<sup>a</sup>

Patient	WHO	Sex	Age,y	Vis F (±)	Probe
1	Recurrent (II)	F	54	+	No
2	I	M	72	+	No
3	II	F	66	+	No
4	Recurrent (II)	M	84	+	No
5	II	F	57	+	No
6	I	M	66	+	Yes
7	I	F	52	+	Yes
8	I	M	46	-	Yes
9	I	F	56	+	Yes
10	I	F	31	+	Yes
11	I	M	80	-	Yes
12	I	M	28	+	Yes
13	I	F	49	-	Yes
14	I	F	46.7	+	Yes
15	I	F	58	+	Yes

<sup>a</sup>Vis F, visible fluorescence; WHO, World Health Organization.

TABLE 2

Quantitative PpIX Levels and Qualitative Fluorescence<sup>a</sup>

Tissue Characteristics	C <sub>PpIX</sub> (mean ± SEM)	C <sub>PpIX</sub> (Minimum Detection Threshold < 0.001: Median and [Min -  Interquartile Range -  Max])
Normal dura	0.006 ± 0.003	<0.001 [0.000 -  0.000-0.000 -  0.0390] <sup>b</sup>
Tumor tissue	1.694 ± 0.44	0.705 [0.000 -  0.066-2.804 -  1.290] <sup>b</sup>
Vis F (-) tissue	0.56 ± 0.022	0.001 [0.000 -  0.000-0.037 -  0.507] <sup>c</sup>
Vis F (+) tissue	2.718 ± 0.631	2.474 [0.000 -  0.731-3.248 -  11.290] <sup>c</sup>
Vis F (-) normal	0.006 ± 0.003	<0.001 [0.000 -  0.000-0.000 -  0.0390]
Vis F (+) tumor	2.718 ± 0.631	2.474 [0.000 -  0.731-3.248 -  11.290]
Vis F (-) tumor	0.118 ± 0.43	0.019 [0.000 -  0.005-0.214 -  0.507]

<sup>a</sup>PpIX, protoporphyrin IX; Vis F, visible fluorescence; SEM, standard error of the mean.

<sup>b</sup>*P* = .002.

<sup>c</sup>*P* < .001.

**TABLE 3**Intraoperative Fluorescence Diagnostics<sup>a</sup>

Diagnostic Metrics	Qualitative Fluorescence (Visible Fluorescence Score $\geq 1$ )	Quantitative Fluorescence	
		C <sub>PpIX</sub> = 0.114 $\mu\text{g/mL}$	C <sub>PpIX</sub> = 0.001 $\mu\text{g/mL}$
Accuracy	0.71	0.84	0.9
PPV	1.00	1.00	0.91
Specificity	1.00	1.00	0.81
NPV	0.55	0.67	0.87
Sensitivity	0.61	0.76	0.94

<sup>a</sup>PpIX, protoporphyrin IX; PPV, positive predictive value; NPV, negative predictive value.